Active Intent Disambiguation for Shared Autonomy Robots

Deepak E. Gopinath and Brenna D. Argall

Abstract—Assistive shared-control robots have the potential to transform the lives of millions of people afflicted with severe motor impairments. The usefulness of shared-control robots typically relies on the underlying autonomy's ability to infer the user's needs and intentions, and the ability to do so unambiguously is often a limiting factor for providing appropriate assistance confidently and accurately. The contributions of this paper are three-fold. First, we propose a goal disambiguation algorithm that enhances the intent inference and assistive capabilities of a shared-control assistive robotic arm. Second, we introduce an intent inference algorithm inspired by dynamic field theory that works in tandem with the disambiguation scheme. Third, we present a pilot study with eight subjects to evaluate the efficacy of the disambiguation algorithm. Our results suggest that (a) the disambiguation system is of greater utility for more limited control interfaces and more complex tasks, and (b) subjects demonstrated a wide range of disambiguation request behaviors with the common thread of concentrating requests early in the execution.

Index Terms—Assistive Robotics, Shared Autonomy, Intent Inference, Intent Disambiguation

I. INTRODUCTION

SSISTIVE and rehabilitation machines—such as robotic arms and smart wheelchairs—have the potential to transform the lives of millions of people with severe motor impairments [1]. With rapid technological advancements in the domain of robotics these machines have become more capable and complex, and with this complexity the control of these machines has become a greater challenge.

The standard usage of these assistive machines relies on manual teleoperation typically enacted through a control interface such as a joystick. However, the greater the motor impairment of the user, the more limited are the interfaces available for them to use. These interfaces (for example, sipand-puffs and switch-based head arrays) are low-dimensional and at times discrete and can typically only operate in subsets of the entire control space (referred to as *control modes*). The dimensionality mismatch between the interface and the robot's controllable degrees-of-freedom (DoF) necessitates the user to switch between control modes during teleoperation and has been shown to add to the cognitive and physical burden and affects task performance negatively [2].

Deepak E. Gopinath is with the Department of Mechanical Engineering, Northwestern University, Evanston, IL and the Shirley Ryan AbilityLab, Chicago, IL.

Brenna D. Argall is with the Departments of Mechanical Engineering, Computer Science and Physical Medicine and Rehabilitation, Northwestern University, Evanston, IL., and the Shirley Ryan AbilityLab, Chicago, IL.

Manuscript received December 2, 2018. Revised on April 21, 2019.

The introduction of *autonomy* to these assistive machines can alleviate some of the above-mentioned issues. More specifically, with *shared* autonomy the task responsibility is shared between the user and the underlying autonomy. However, for autonomy to be effective in a shared setting, it needs to have a good idea of the user's needs and intentions. That is, *intent inference* is critical to ensure appropriate assistance.

In this work, we consider use-case scenarios in which the autonomy's inference of user intent is exclusively informed by the human's control commands issued via the control interface. As an example, in the domain of assistive robotic manipulation, these control commands are typically mapped to the end-effector (or joint) velocities and results in robot motion. Motion carries information regarding underlying intent. However, intent inference becomes particularly challenging when the user input is low-dimensional and sparse, as is the case with the more limited interfaces available to those with severe motor impairments. This is due to the fact that robot motion will likely be more discontinuous and jagged, and it might not carry information regarding underlying human intent. While to augment the human-robot system with high-fidelity sensors could be a straightforward approach to enhance the autonomy's intent inference capabilities in the assistive domain, user satisfaction and comfort is of paramount importance; furthermore additional sensors can quickly become cumbersome (e.g., if the sensors have to be worn by the user) and expensive. Therefore, for reasons of user adoption and cost, we intentionally design our assistance add-ons to be as invisible and close to the manual system as possible. The need for intent (goal) disambiguation arises as the autonomy needs to reason about all possible goals before issuing appropriate assistance commands.

Our key insight in this work is that certain user control commands issued in certain control modes are *more intent expressive* than others and therefore may help the autonomy to improve inference accuracy. More specifically, in this work we investigate how the selection of a subset of the operational control dimensions or modes improves the intent inference and disambiguation capabilities of the robot. The three main contributions of this work are as follows:

1) First, we develop a control mode selection algorithm which selects the control mode for the user, in which the user-initiated motion will help the autonomy to maximally disambiguate human intent by eliciting more intent expressive control commands from the human. In doing so, the autonomy will likely be able to assist the human more effectively and thereby improve overall task performance. This is important especially in the

domain of assistive robotics wherein the user control commands are typically low-dimensional and sparse due to the inherent limitations of the control interfaces.

- 2) Second, as the disambiguation power of our algorithm is closely linked to the fidelity of the underlying intent inference mechanism, we also propose a novel intent inference scheme based on ideas from *dynamic field* theory in which the time evolution of the probability distribution over goals is specified as continuous-time constrained dynamical system.
- 3) Third, we present results from a pilot study conducted to evaluate the efficacy of the disambiguation algorithm.

In Section II we present an overview of relevant research in the areas of shared autonomy in assistive robotics, intent inference, and synergies in human-robot interaction. Section III presents our mathematical formalism developed for intent disambiguation and inference. The study design and experimental methods are discussed in Section V followed by results in Section VI. Discussion and conclusions are presented in Sections VII and VIII.

II. RELATED WORK

This section provides an overview of related research in the domains of shared autonomy in assistive robotics, intent inference in human-robot interaction, and synergies in humanrobot interaction.

Shared-autonomy in assistive systems aims to reduce the user's cognitive and physical burden during task execution, typically without having the user relinquish complete control [3], [4], [5], [6]. In order to offset the drop in task performance due to shifting focus (task switching) from the task at hand to switching between different control modes, various mode switch assistance paradigms have been proposed. For example, a simple time-optimal mode switching scheme has shown to improve task performance [2], [7].

Shared control systems often require a good estimate of the human's intent—for example, their intended reaching target in a manipulation task or a target goal location in a navigation task [8]. Intent can be explicitly communicated by the user [9] via various modalities such as laser pointers, click interfaces and in some cases natural language. Intent can also be inferred from the user's control signals and other environmental cues using various algorithms. Within the context of shared autonomy a Bayesian scheme for user intent prediction models the user within the Markov Decision Process framework [10], [11], [12] and is typically assumed to be noisily optimizing some cost function for their intended goal. In low-dimensional spaces, this cost function can be learned from expert demonstrations using Inverse Reinforcement Learning [13].

For high-dimensional spaces, such as that of robotic manipulation, learning cost functions that generalize well over the entire space requires large number of samples. In such cases, heuristic cost functions, such as sum of squared velocities along a trajectory, have been found to be useful for goal prediction [14]. Simple heuristic approaches can also be used to find direct mappings from instantaneous cues and the underlying human intention. Heuristic approaches can

incorporate domain-specific knowledge easily and are computationally inexpensive, though the trade-off of this simplicity is not being sophisticated enough to incorporate histories of states and actions, making them less robust to external noise. Instantaneous confidence functions for estimating the intended reaching target are employed with success on multiple robotic manipulation systems [15], [5]. In our work we develop an inference algorithm that updates the belief over goals using ideas from dynamic field theory in which the histories of states and actions are incorporated using a single time-scale parameter and robustness to noise is ensured via recurrent self-interactions that stabilizes the dynamical system.

From the robot's perspective, the core idea behind our intent disambiguation system is that of "Help Me, Help You"—that is, if the user can help the robot with more intent-expressive actions, then the robot in turn can provide accurate and appropriate task assistance more accurately and confidently. More intent-expressive human actions also is related to the idea of legibility in robot actions. In human-robot interaction, the legibility and predictability of robot motion to the human is investigated [16] with various techniques to generate legible robot motion proposed [17]. Our work relies on the idea of inverse legibility [18] in which the assistance scheme is intended to bring out more legible intent-expressive control commands from the human.

III. MATHEMATICAL FORMALISM FOR INTENT DISAMBIGUATION

This section describes our intent disambiguation algorithm, that computes the control mode that can maximally disambiguate between the goals, and our intent inference mechanism that works in conjunction with disambiguation algorithm.

A. Notation

Let $\mathcal G$ denote the set of all candidate goals with $n_g=|\mathcal G|$ and let g^i refer to the i^{th} goal with $i\in[1,2,\ldots,n_g].$ A goal in this context represents the human's underlying intent. Specifically, in assistive robotic manipulation, since the robotic device first must reach toward and grasp discrete objects in the environment, intent inference is the estimation of the probability distribution over all possible discrete goals (objects) in the environment. At any time t, the autonomy maintains a probability distribution over goals denoted by p(t) such that $p(t) = [p^1(t), p^2(t), \ldots, p^{n_g}(t)]^T$ where $p^i(t)$ denotes the probability associated with goal g^i . The probability $p^i(t)$ represents the robot's confidence that goal g^i is the human's intended goal. $p^i(t)$

Let K be the set of all controllable dimensions of the robot and k^i represent the i^{th} control dimension where

¹By having the autonomy maintain a probability distribution over goals, we implicitly model the human as a Partially Observable Markov Decision Process (POMDP) in which all the uncertainty in the user's state is concentrated in the user's intended goal. By maintaining and updating a probability distribution over goals the autonomy can reason about the human's latent state (internal goal) during trial execution. Inference over goal states is typically done using recursive Bayesian belief update which determines how the distribution evolves over time. In Section IV we introduce a novel approach to compute the time evolution of probability distribution over goals that serves as an alternative to the recursive Bayesian update scheme.

3

 $i \in [1,2,\ldots,n_k]$ with $n_k = |\mathcal{K}|$. The limitations of the control interface necessitates \mathcal{K} to be partitioned into control modes. Let \mathcal{M} denote the set of all control modes with $n_m = |\mathcal{M}|$. Additionally, let m^i refer to the i^{th} control mode where $i \in [1,2,\ldots,n_m]$. Each control mode m^i is a subset of \mathcal{K} such that $\bigcup_{i=1}^{n_m} m^i$ spans all of the controllable dimensions. A dimension $k \in \mathcal{K}$ can be an element of multiple control modes.

In this work, we assume a kinematic model for the robot and the kinematic state (the robot's end-effector pose) at any time t is denoted as $\boldsymbol{x}_r(t) \in \mathbb{R}^3 \times \mathbb{S}^3$ and consists of a position and orientation component, where \mathbb{S}^3 is the space of all unit quaternions. The pose for goal $g \in \mathcal{G}$ is denoted as $\boldsymbol{x}_g \in \mathbb{R}^3 \times \mathbb{S}^3$. The control command issued by the human via the control interface is denoted as \boldsymbol{u}_h and is mapped to the Cartesian velocity of the robot's end-effector. For a 6-DoF robotic arm, $\boldsymbol{u}_h \in \mathbb{R}^6$. The autonomous robot control policy that generates a robot control command is denoted as $\boldsymbol{u}_r \in \mathbb{R}^6$. The control command issued to the robot, which is a synthesis of \boldsymbol{u}_h and \boldsymbol{u}_r is denoted as $\boldsymbol{u} \in \mathbb{R}^6$. The control command that corresponds to a unit velocity vector along the positive and negative directions of control dimension k is denoted as e^k and e^k respectively.

B. Disambiguation Metric

The disambiguation metric that we develop in this paper is a heuristic measure that characterizes the intent disambiguation capabilities of a control dimension $k \in \mathcal{K}$ and is denoted as $D_k \in \mathbb{R}$. We explicitly define disambiguation metrics for both positive and negative motions along k as D_k^+ and $D_k^$ respectively. We also define a disambiguation metric $D_m \in \mathbb{R}$ for each control mode $m \in \mathcal{M}$. By virtue of design, the disambiguation metric D_m is a measure of how useful the user control commands would be for the robot to perform more accurate intent inference if the user were to operate the robot in control mode m. Both D_k and D_m will be formally defined in Section III-D. Our computation of D_k depends on four features (denoted as Γ_k , Ω_k , Λ_k and Υ_k), that capture different aspects of the shape of a projection of the probability distribution over intent. These projections and computations are described in detail in Section III-C and Section III-D, and as pseudocode in Algorithm 1.

C. Forward Projection of p(t)

The first step towards the computation of D_k is model-based forward projection of the probability distribution p(t) from the current time t_a to t_b and t_c (Algorithm 1, lines 4-5) where $t_a < t_b < t_c$. We consider two future times in order to compute short-term (t_b) and long-term (t_c) evolutions of the probability distribution. Application of e^k results in probability distributions $p_k^+(t_b)$, $p_k^+(t_c)$ and $-e^k$ results in $p_k^-(t_b)$ and $p_k^-(t_c)$, where the subscript k captures the fact that the projection is the result of the application of a control command only along control dimension k. All parameters which affect the computation of p(t) are denoted as Θ .

Algorithm 1 Intent Disambiguation

```
Require: p(t_a), x_r(t_a), \Delta t, t_a < t_b < t_c, \Theta
  1: for k = 0 \dots n_k do
          Initialize D_k = 0, t = t_a, \boldsymbol{u}_h = \boldsymbol{e}^k
          while t \leq t_c do
  3:
  4:
              \boldsymbol{p}_k(t+\Delta t) \leftarrow \text{UpdateIntent}(\boldsymbol{p}_k(t), \boldsymbol{u}_h; \boldsymbol{\Theta})
              \boldsymbol{x}_r(t + \Delta t) \leftarrow \text{SimulateKinematics}(\boldsymbol{x}_r(t), \boldsymbol{u}_h)
 5:
  6:
              if t = t_b then
  7:
                  Compute \Gamma_k, \Omega_k, \Lambda_k
  8:
              end if
  9:
              if t = t_c then
                  Compute \Upsilon_k
10:
11:
              end if
12:
              t \leftarrow t + \Delta t
          end while
13:
14:
          Compute D_k
15: end for
```

D. Features of D_k

To compute our disambiguation metric, we design four features that encode different aspects of the *shape* of the probability distribution as it evolves under user control in a specific control dimension k. For each control dimension k, each of the four features is computed for projections along both positive and negative directions independently. The four features are computed in lines 7 and 10 in Algorithm 1.

1) Maximum: The maximum of the projected probability distribution $p_k(t_b)$ is a good measure of the robot's overall certainty in accurately predicting human intent. We define the distribution maximum as

$$\Gamma_k = \max_{1 \le i \le n_q} p_k^i(t_b) \tag{1}$$

(i.e., the mode of this discrete distribution). A higher value implies that the robot has a greater confidence in its prediction of the human's intended goal.

2) Pairwise separation: More generally, disambiguation accuracy benefits from a larger separation, Λ_k , between goal probabilities. The quantity Λ_k is computed as the *sum of the pairwise distances* between the n_q probabilities.

$$\Lambda_k = \sum_{i=1}^{n_g} \sum_{j=i}^{n_g} |p_k^i(t_b) - p_k^j(t_b)|$$
 (2)

 Λ_k is particularly helpful if the difference between the largest probabilities fails to disambiguate.

3) Difference between maxima: Disambiguation accuracy benefits from greater differences between the first and second most probable goals. This difference is denoted as

$$\Omega_k = \max(\boldsymbol{p}_k(t_b)) - \max(\boldsymbol{p}_k(t_b) \setminus \max(\boldsymbol{p}_k(t_b)))$$
 (3)

 Ω_k becomes particularly important when the distribution has multiple modes and a single measure of maximal certainty (Γ_k) alone is not sufficient for successful disambiguation.

4) Gradients: Γ_k , Ω_k and Λ_k are local measures that encode shape characteristics of the short-term temporal projections of the probability distribution over goals. However, the quantity

²UpdateIntent() in Line 4 is implemented using Equation 6 discussed in detail in Section IV-B and SimulateKinematics() assumes a point-like robot kinematics.

 $\boldsymbol{p}_k(t)$ can undergo significant changes upon long-term continuation of motion along control dimension k. The spatial gradient of $\boldsymbol{p}_k(t)$ encodes this propensity for change and is approximated by

$$\frac{\partial \boldsymbol{p}_k(t)}{\partial x_k} \simeq \frac{\boldsymbol{p}_k(t_c) - \boldsymbol{p}_k(t_b)}{x_k(t_c) - x_k(t_b)}$$

where x_k is the component of robot's projected displacement along control dimension k. The greater the difference between individual spatial gradients, the greater will the probabilities deviate from each other, thereby helping in disambiguation. In order to quantify the "spread" of gradients we define Υ_k as

$$\Upsilon_k = \sum_{i=1}^{n_g} \sum_{j=i}^{n_g} \left| \frac{\partial p_k^i(t)}{\partial x_k} - \frac{\partial p_k^j(t)}{\partial x_k} \right| \tag{4}$$

where |.| denotes the absolute value.

5) Putting it all together: The individual features Γ_k , Ω_k , Λ_k and Υ_k are combined to compute D_k in such a way that, by design, higher values of D_k imply greater disambiguation capability for the control dimension k. More specifically,

$$D_k = \underbrace{w \cdot (\Gamma_k \cdot \Lambda_k \cdot \Omega_k)}_{\text{short-term}} + \underbrace{(1 - w) \cdot \Upsilon_k}_{\text{long-term}}$$
(5)

where w is a task-specific weight that balances the contributions of the short-term and long-term components (in our implementation, w is empirically set to 0.5). Equation 5 is computed twice, once in each of the positive (e^k) and negative directions $(-e^k)$ along k, and the results (D_k^+) and $D_k^-)$ are then summed to compute D_k .

The computation of D_k is performed for each control dimension $k \in \mathcal{K}$. The disambiguation metric D_m for control mode m then is calculated as

$$D_m = \sum_{k \in m} D_k$$

and the control mode with highest disambiguation capability m^* is given by

$$m^* = \operatorname*{argmax}_m D_m$$

while $k^* = \operatorname{argmax}_k D_k$ gives the control dimension with highest disambiguation capability k^* . Disambiguation mode m^* is the mode that the algorithm chooses for the human to better estimate their intent.

IV. INTENT INFERENCE

In this section, we propose a novel intent inference scheme inspired by dynamic field theory in which the time evolution of the probability distribution p(t) is specified as a dynamical system with constraints. Section IV-A provides a primer on the basic principles and features of dynamic field theory and its application in the fields of neuroscience and cognitive robotics. Section IV-B describes our novel formulation that makes use of dynamic field theory for the purposes of intent inference.

A. Dynamic Field Theory

In Dynamic Field Theory (DFT) [19], variables of interest are treated as dynamical state variables. To represent the information about these variables requires two dimensions: one which specifies the value the variables can attain (the domain) and the other which encodes the *activation level* or the amount of information about a particular value. These *activation fields* (also known as dynamic neural fields) are analogous to probability distributions defined over a random variable.

Following Amari's formulation [20] dynamics of an activation field $\phi(x,t)$ are given by

$$\tau \frac{\partial \phi(x,t)}{\partial t} = -\phi(x,t) + h + S(x,t) + \int dx' b(x-x') \sigma(\phi(x',t))$$

where x denotes the variable of interest, t is time, τ is the timescale parameter, h is the constant resting level, and S(x,t) is the external input, b(x-x') is the interaction kernel and $\sigma(\phi)$ is a sigmoidal nonlinear threshold function. The interaction kernel mediates how activations at all other field sites x' drive the activation level at x. Two types of interactions are possible: excitatory (when interaction is positive) which drives up the activation, and inhibitory (when the interaction is negative) which drives the activation down. Historically, dynamic neural fields originally were conceived to explain cortical population neuronal dynamics, based on the hypothesis that the excitatory and inhibitory neural interactions between local neuronal pools form the basis of cortical information processing [21]. These activation fields possess some unique characteristics that make them ideal candidates for modeling higher-level cognition. First, a peak in the activation field can be sustained even in the absence of external input due to the recurrent interaction terms. Second, information from the past can be preserved over much larger time scales quite easily by tuning the time-scale parameter thereby endowing the fields with memory. Third,

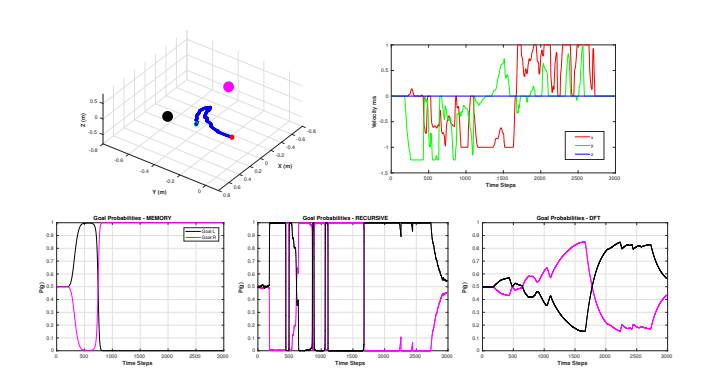


Fig. 1. Goal inference comparison: (Top Row, Left). The two goals are depicted as black and magenta circles. The robot end-effector trajectory is colored in blue and the start and end points are marked as red and green respectively. (Top Row, Right). The user control command profile for translational dimensions. (Bottom Row, Left to Right). Goal probabilities for Memory-Based Prediction (Left), Recursive Bayesian Belief Update (Middle) and DFT-based inference scheme (Right).

5

the activation fields are *robust* to disturbance and noise in the external input [22].

B. Dynamic Neural Fields for Intent Inference

Recurrent interaction between the state variables, robustness to noise, and inherent memory make dynamic neural fields an ideal candidate for an intent inference engine. Our insight is to use the framework of dynamic neural fields to specify the time evolution of the probability distribution p(t), in which we treat the individual goal probabilities $p^i(t)$ as constrained dynamical state variables such that $p^i(t) \in [0,1]$ and $\sum_{1}^{n_g} p^i(t) = 1$. The dynamical system can be generically written as

$$\frac{\partial \boldsymbol{p}(t)}{\partial t} = F(\boldsymbol{p}(t), \boldsymbol{u}_h; \boldsymbol{\Theta})$$

where F represents the nonlinear vector field, u_h is the human control input and Θ represents all other task-relevant features and parameters that affect the time-evolution of the probability distribution.

The full specification of the neural field is given by

$$\frac{\partial \boldsymbol{p}(t)}{\partial t} = \frac{1}{\tau} \left[-\mathbb{I}_{n_g \times n_g} \cdot \boldsymbol{p}(t) + \underbrace{\frac{1}{n_g} \cdot \mathbb{1}_{n_g}}_{\text{rest state}} \right] + \underbrace{\boldsymbol{\lambda}_{n_g \times n_g} \cdot \sigma(\boldsymbol{\xi}(\boldsymbol{u}_h; \boldsymbol{\Theta}))}_{\text{excitatory + inhibitory}}$$
(6)

where u_h is the human control input and Θ represents all other task-relevant features, time-scale parameter τ determines the memory capacity, $\mathbb{I}_{n_g \times n_g}$ is the identity matrix, \mathbb{I}_{n_g} is a vector of dimension n_g containing all ones, λ is the control matrix that controls the excitatory and inhibitory aspects, ξ is a function that encodes the nonlinearity through which human control commands and task features affect the time evolution, and σ is a biased sigmoidal nonlinearity given by $\sigma(\xi) = \frac{1}{1+e^{-\xi}} - 0.5$. The key adaptation required to use DFT for intent inference is in the design of ξ .

Our design of ξ is informed by what features of the human control input and environment effectively capture the human's underlying intent. We choose the *directedness* of the robot motion towards a goal, the *agreement* between the human commands and robot autonomy, and the *proximity* to a goal. The *directedness* component looks at the shortest straight line path towards a goal g, whereas the *agreement* serves as an indicator of how similar (measured as a dot product) the human and autonomy signals are to each other. One dimension i of ξ is defined as

$$\begin{split} \xi^{i}(\boldsymbol{u}_{h}; \boldsymbol{x}_{r}, \boldsymbol{x}_{g^{i}}, \boldsymbol{u}_{r,g^{i}}) &= \underbrace{\frac{1+\eta}{2}}_{\text{directedness}} + \underbrace{\boldsymbol{u}_{h}^{rot} \cdot \boldsymbol{u}_{r,g^{i}}^{rot}}_{\text{agreement}} \\ &+ \underbrace{\max \Big(0, 1 - \frac{\left\|\boldsymbol{x}_{g^{i}} - \boldsymbol{x}_{r}\right\|}{R}\Big)}_{\text{proximity}} \end{split}$$

where $\eta = \frac{ \mathbf{u}_h^{trans} \cdot (\mathbf{x}_{g^i} - \mathbf{x}_r)^{trans} }{\|\mathbf{u}_h^{trans}\|\|(\mathbf{x}_{g^i} - \mathbf{x}_r)^{trans}\|}, \ \mathbf{u}_{r,g^i}$ is the robot autonomy command for reaching goal g^i , trans and rot refer to the translational and rotational components of a command \mathbf{u}

or position x, R is the radius of the sphere beyond which the proximity component is always zero, $\|\cdot\|$ is the Euclidean norm and $\Theta = \{x_r, x_{g^i}, u_{r,g^i}\}$. At every time-step constraints on $p^i(t)$ are enforced such that p(t) is a valid probability distribution. The most confident goal g^* is computed as $g^* = \operatorname{argmax}_i p^i(t)$.

C. Qualitative Comparison of Goal Inference Methods

Figure 1 shows an illustrative comparison of goal inferences using our DFT-based approach and two other Bayesian approaches i) memory-based prediction as implemented in [14] and ii) recursive belief updating as implemented in [23].³

In the scenario shown in Figure 1 (top row), the user teleoperates the end-effector in the three translational dimensions. The user initially moves the robot towards the black goal (on the left) and then changes direction to pursue the magenta goal (on the right). Subsequently, the user decides against going towards the magenta goal and decides to pursue the initial black goal by moving the end-effector to the left.

In Figure 1 we can see that (bottom row) the goal probabilities under our DFT-based inference mechanism evolve much more smoothly compared to the recursive belief update scheme thereby decreasing the possibility of false positives. Moreover, it is able to capture the change in user's intention back to the original goal and outperforms the memory-based prediction scheme. The choice of cost functions and likelihood functions have a significant impact on the performance of the memory-based and recursive belief update inference schemes. Overall the performance of DFT-based inference schemes are comparable to standard Bayesian approaches.

V. STUDY METHODS

In this section, we describe the study methods used to evaluate the efficacy of the disambiguation system.

Participants: For this study eight subjects were recruited $\overline{\text{(mean age: }31\pm11, 3 \text{ males and 5 females)}}$. All participants gave their informed, signed consent to participate in the experiment, which was approved by Northwestern University's Institutional Review Board.

Hardware: The experiments were performed using the MICO 6-DoF robotic arm (Kinova Robotics, Canada), specifically designed for assistive purposes. The software system was implemented using the Robot Operating System (ROS) and data analysis was performed in MATLAB. The subjects teleoperated the robot using two different control interfaces: a 2-axis joystick and a switch-based head array, controlling the 6D Cartesian velocities of the end-effector (Figure 2). An external button was provided to request the mode switch assistance.

In detail, the joystick generated 2D continuous control signals. Under joystick control the full control space was partitioned into five control modes that were accessed via button presses. The switch-based head array consisted of three switches embedded in the headrest, operated via head

 $^3 \mathrm{For}$ the memory-based inference scheme we use a straight-line distance based cost function and for the recursive belief update scheme we model the human as an approximately rational agent such that the $p(\boldsymbol{u}_h|g)$ is modeled as a von Mises distribution.

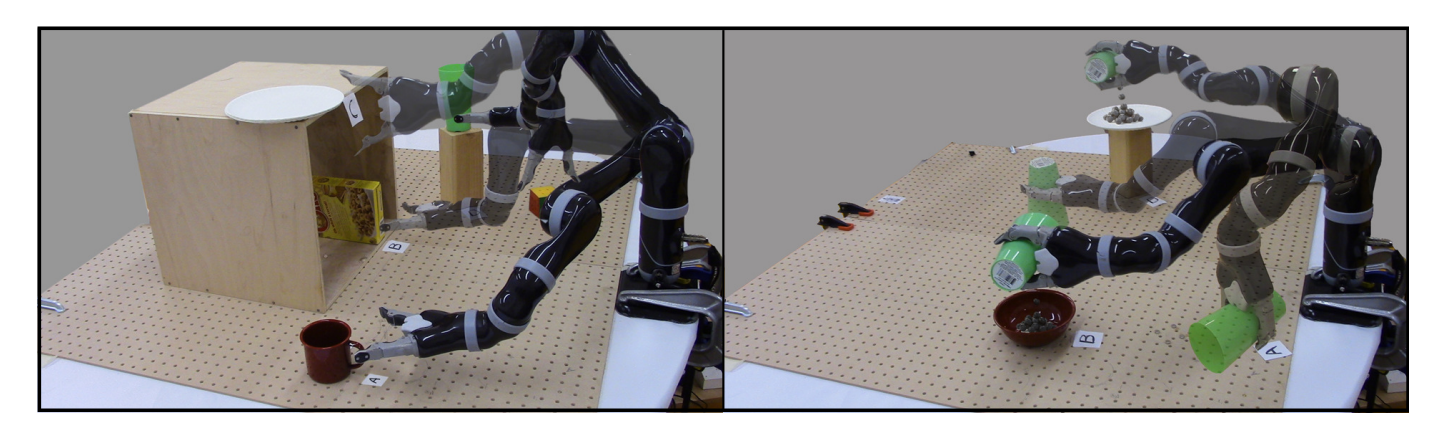


Fig. 3. Study tasks performed by subjects. Left: Single-step reaching task. Right: Multi-step pouring task.

movements and generated 1D discrete signals. Under head array control the full control space was partitioned into seven control modes, the back switch was used to cycle between the different control modes, and the switches to the left and right controlled the motion of the robot's end effector in the positive and negative directions along a selected control dimension.

Tasks: Two different task types were evaluated.

Single-step: The aim was to reach one of five objects on the table, each with a target orientation (Figure 3, Left).

<u>Multi-step:</u> Each trial began with a full cup held by the robot gripper. The task required first that the contents of the cup be poured into one of two containers, and then that the cup be placed at one of the two specified locations and with a specific orientation (Figure 3, Right).

Switching Paradigms: Two kinds of mode switching paradigms were evaluated in the study.

<u>Manual</u>: During task execution the user performed all mode switches.

<u>Disambiguation</u>: The user either performed a mode switch manually or requested a switch to a *disambiguation* mode. The user was free to issue disambiguation requests at any time during task execution, upon which the algorithm identified and switched the current control mode to the best disambiguating mode m^* by invoking Algorithm 1. It has to be noted that the user was also allowed to switch control modes using a manual mode switch any time as well. However, the user was required to request disambiguation at least once during the task execution.

Shared Control: Autonomy assistance was always active for



Fig. 2. A 2-axis joystick (left) and switch-based head array (center) and their operational paradigms (right). v and ω indicate the translational and rotational velocities of the end-effector, respectively.

both mode switch assistance (manual and disambiguation) paradigms. We used a blending-based shared-control paradigm in which the final robot control command was a linear composition of the human control command and an autonomous robot policy. With blending the amount of assistance was directly proportional to the probability of the most confident goal g^* , and thus to the strength of the intent inference. The probability distribution over goals, p(t), was updated using Equation 6 outlined in Section IV-B and the most confident goal was computed as $\arg\max_i p^i(t)$ Therefore, if intent inference improved as a result of goal disambiguation, more assistance would be provided by the robot.

Specifically, the autonomous control policy generates control command $u_r \leftarrow f_a(x_r)$ where $f_a(\cdot) \in \mathcal{F}_a$, and \mathcal{F}_a was the set of all control behaviors corresponding to different tasks. This set could be derived using a variety of techniques such as *Learning from Demonstrations* [24], [25], motion planners [26], [27] or navigation functions [28], [29]. In our implementation, the autonomy's control command was generated using a simple potential field which is defined in all parts of the state space [30]. Every goal g was associated with a potential field γ_g which treats g as an attractor and all the other goals in the scene as repellers. The autonomy command was computed as a summation of the attractor and repeller velocities and operated in the full 6D Cartesian space.

Let $u_{r,g}$ be the autonomy command associated with goal g. Under blending, the final control command u issued to the robot then was given by

$$\boldsymbol{u} = \alpha \cdot \boldsymbol{u}_{r,q^*} + (1 - \alpha) \cdot \boldsymbol{u}_h$$

where g^* was the most confident goal. Similar to u_h , the autonomy command $u_{r,g^*} \in \mathbb{R}^6$ is mapped to the 6D Cartesian velocity of the end-effector. The blending factor α was a piecewise linear function of the probability $p(g^*)$ associated with g^* and was given by

$$\alpha = \begin{cases} 0 & p(g^*) \le \rho_1 \\ \frac{\rho_3(p(g^*) - \rho_1)}{\rho_2 - \rho_1} & \text{if } \rho_1 < p(g^*) \le \rho_2 \\ \rho_3 & p(g^*) > \rho_2 \end{cases}$$

with $\rho_i \in [0,1] \ \forall \ i \in [1,2,3]$ and $\rho_2 > \rho_1$. In our implementation, we empirically set $\rho_1 = \frac{1.2}{n_g}, \rho_2 = \frac{1.4}{n_g}$ and $\rho_3 = 0.7$.

<u>Study protocol</u>: A within-subjects study was conducted using a fractional factorial design in which the manipulated variables were the tasks, control interfaces and the switching paradigm conditions. Each subject underwent an initial training period that lasted approximately 30 minutes.

The training period consisted of three phases and two different task configurations. The subjects used both interfaces to perform the training tasks.

<u>Phase One</u>: The subjects were asked to perform a simple reaching motion towards a single goal in the scene. This phase was intended for the subjects to get familiarized with the control interface mappings and teleoperation of the robotic arm.

<u>Phase Two</u>: In the second phase of training, subjects experienced how the blending-based autonomy provided assistance during task execution.

<u>Phase Three</u>: For the third phase of the training, multiple objects were introduced in the scene. Subjects were able to explore the disambiguation request feature during a reaching task, to observe the effects of the mode switch request and subsequent change in robot assistance. Subjects were explicitly informed by the experimenter that upon a disambiguation request the robot will select a control mode that would help the autonomy figure out which goal the subject was going for and thereby enable it to assist the user more effectively.

During the testing phase, each subject performed both tasks using both interfaces under the *Manual* and *Disambiguation* paradigms. All trials started in a randomized initial control mode and robot position. The ordering of control interfaces and paradigms was randomized and counterbalanced across all subjects. Three trials were collected for the *Manual* paradigm and five trials for the *Disambiguation* paradigm. Each trial lasted approximately 10-40s depending on the starting position of the robot and the specified reaching target. At the start of each trial, p(t) was initialized as $\frac{1}{n_g} \cdot \mathbb{1}_{n_g}$. During the trial as the user teleoperated the robot by generating control commands using the specified control interface, p(t) was updated according to Equation 6 in an online fashion at each time step. Figure 4 captures how a single trial unfolds in time. **Metrics:** The objective metrics used for evaluation included the following.

- *Number of mode switches*: The number of times a user switched between various control modes during task execution. This metric captures one of the main factors that contributes to the cognitive and physical effort required for task execution in assistive robotic manipulation [2].
- *Number of disambiguation requests*: The number of times user pressed the disambiguation request button.
- Number of button presses: The sum of Number of mode switches and Number of disambiguation requests.
- Skewness: A higher-order moment used to quantify the asymmetry of any distribution. Used to characterize how much the temporal distribution of disambiguation requests deviates from a uniform distribution.

VI. RESULTS

Here we report the results of our subject study. Our study results indicated that the disambiguation request system is of

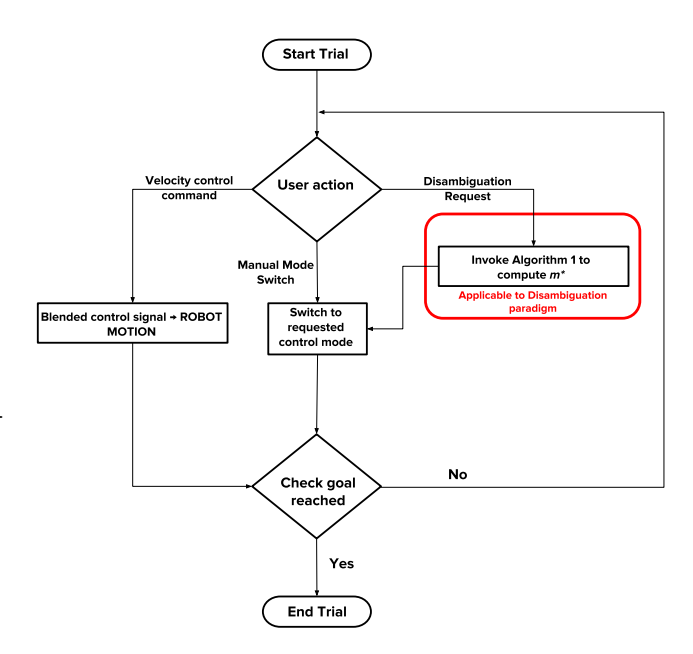


Fig. 4. Flow chart depicting user action sequence during a single trial. The user can issue three types of actions: a) Velocity control command b) Manual mode switch using a button press and c) Disambiguation request using a button press. Option a) results in online intent inference followed by generation of autonomy signal and blended control signal and subsequently causes robot motion. Options b) and c) lead to a control mode switch. At every timestep, the autonomy checks for the goal condition and decides whether to terminate the trial or not.

greater utility for more limited control interfaces and more complex tasks and subjects demonstrated a wide range of disambiguations request behaviors with a common theme of relying on disambiguation assistance early in the trials. Statistical significance was determined by the Wilcoxon Rank-Sum test in where (***) indicates p < 0.001, (**) p < 0.01 and (*) p < 0.05.

Impact of Disambiguation on Task Performance: A statistically significant decrease in the number of button presses was observed between the *Manual* and *Disambiguation* paradigms when using the headarray (Figure 5, Left). Due to the low-

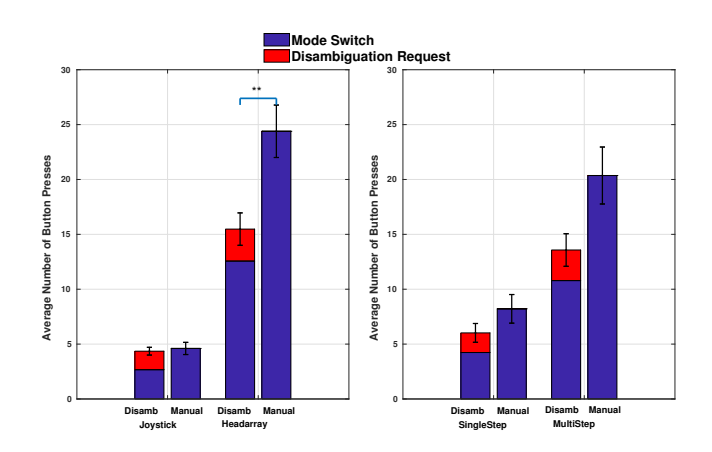


Fig. 5. Comparison of average number of button presses between *Disambiguation* and *Manual* Paradigms. *Left:* Grouped by control interfaces. *Right:* Grouped by tasks.

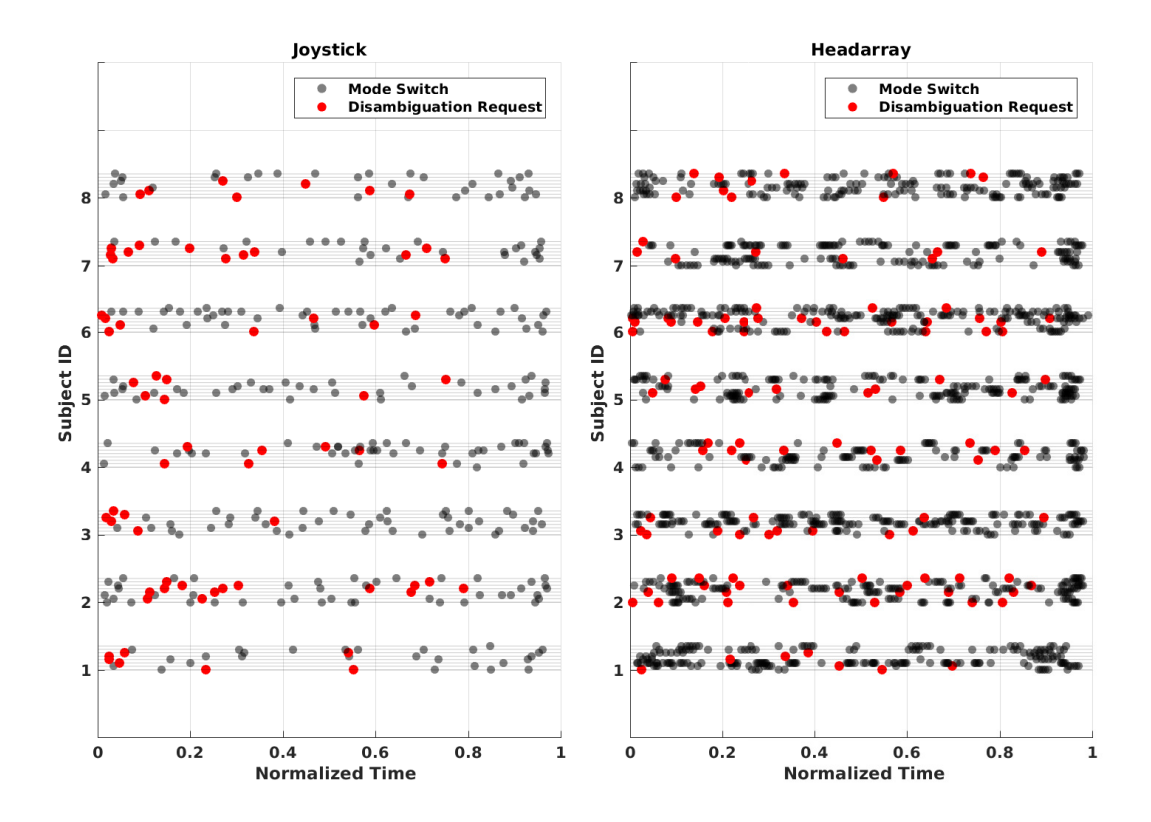


Fig. 6. Temporal pattern of button presses for each interface and the multi-step task on a trial-by-trial basis for all subjects. Eight trials per subject per interface/task combination. For each subject, each light gray horizontal line represents a single trial (8 trials in total).

dimensionality of the headarray and cyclical nature of mode switching, the number of button presses required for task completion is inherently high. That the disambiguation paradigm was helpful in reducing the number of button presses likely is due to higher robot assistance in the disambiguating control mode and therefore reduced the need for subsequent user-initiated mode switches. For the joystick, statistically significant differences between the two paradigms were observed for the number of manual mode switches (p < 0.05). However, this gain was offset by the button presses that were required for disambiguation requests. When grouping by task, the general trend (although not statistically significant) of a decrease in the number of button presses was more pronounced for the more complex multi-step task (Figure 5, Right).

These results suggest that disambiguation is more useful as the control interface becomes more limited and the task becomes more complex. Intuitively, intent prediction becomes harder for the robot when the control interface is low-dimensional and does not reveal a great deal about the user's underlying intent. By having the users operate the robot in the disambiguating mode, the robot is able to elicit more intent-expressive control commands from the human which in turn helps in accurate goal inference and subsequently appropriate robot assistance.

Temporal Distribution of Disambiguation Requests: The temporal distribution of disambiguation requests refers to *when* the subject requested assistance during the course of a trial.

We observed that a higher number of disambiguation requests correlates with the more limited interface and complex task.

From Figure 6 it is clear that the frequency and density of button presses (disambiguation requests plus mode switches) are much higher for the more limited control interface. The subjects also demonstrated a diverse range of disambiguation request behaviors, for example in regards to both when during the execution requests were made and with what frequency (e.g., Subject 8 versus Subject 2, Joystick). The variation between subjects is likely due to various factors such as the user's comfort in operating the robot and understanding of the disambiguating mode's ability to recruit more assistance from the autonomy. The skewness of the temporal distribution of disambiguation requests revealed a higher concentration of during the earlier parts of a trial (Table I) for both interfaces and tasks. However, under headarray control the temporal distribution was less skewed as the need for disambiguation request persists throughout the trial due the extremely low-

TABLE I
CHARACTERIZATION OF THE TEMPORAL DISTRIBUTION OF
DISAMBIGUATION REQUESTS.

	Single Step	Multi Step
Joystick	0.63	0.57
Headarray	0.35	0.22

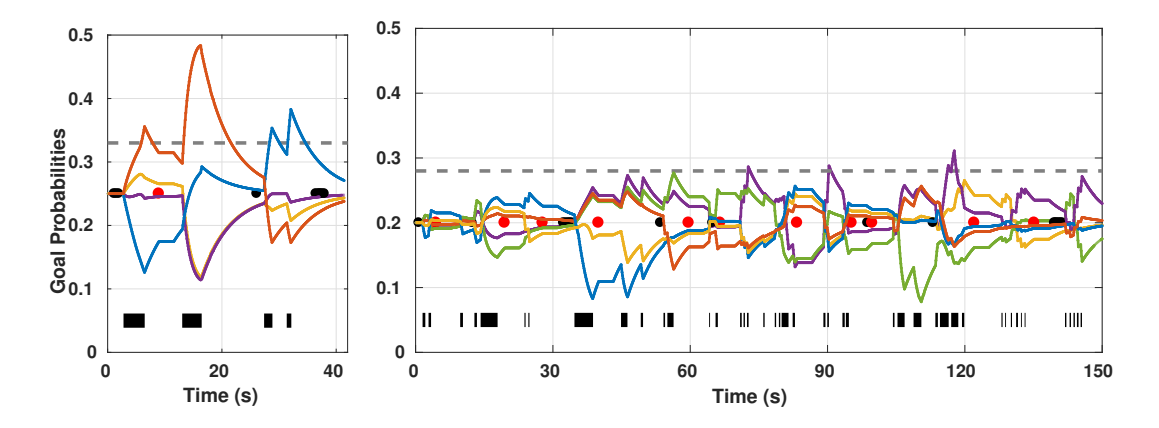


Fig. 7. Time evolution of goal probabilities. *Top:* Multi-step task. *Bottom:* Single-step task. The gray horizontal dashed line above denotes the minimum threshold for robot assistance. The black horizontal bars at the bottom denote non-zero human control commands. The red and black dots indicate button presses that are disambiguation requests and mode switches respectively.

bandwidth of the interface.4

VII. DISCUSSION

The disambiguation algorithm presented in our work can be utilized in any human-robot system in which there is a need to disambiguate between the different states a discrete hidden variable can assume (for example, a discrete set of goals in robotic manipulation or a set of landmarks in navigation tasks). Our algorithm assumes the existence of a discrete set of parameters (for example, control modes for robotic manipulation or natural language-based queries for navigation) that can help the intent inference mechanism to precisely converge to the correct inference. Although the disambiguation algorithm is task-agnostic-because it relies exclusively on the shape features of the probability distribution over the hidden variable—the disambiguation is only as good as the efficacy of the intent inference algorithm that is used for as specific task. In our experience, it becomes important that the choice of cost functions and domain-specific heuristics is appropriate for the task at hand.

The efficacy of the disambiguation algorithm degraded when we used only a subset of the four features to inform the disambiguation metric. This only reinforces the need for a combination of different shape features for successful disambiguation.

One observation from our subject study was how often participants submitted a disambiguation request and then chose not to operate in the selected mode—effectively not letting the robot help them. Our preliminary analysis showed that even though the autonomy was in a control mode that could have helped it perform accurate intent inference and subsequently assist the human, the user was not able to capitalize on it and utilize it to his/her advantage. As a result no differences in the onset of assistance was observed between the two switching paradigms across tasks or across interfaces. This phenomenon

⁴A uniform temporal distribution corresponds to a trial in which the disambiguation requests are uniformly spread out during the course of task execution. The skewness of a uniform distribution of 0.

is illustrated in Figure 7. When control commands are issued, they are indicated by the black horizontal bars at the bottom of the plots. Disambiguation requests are shown as red dots, and mode switches as black dots. In plot on the right, we see multiple instances of disambiguation requests followed by no control commands or only very brief control commands. Another interesting behavior is shown in the left plot, where operation in the disambiguating mode very quickly elevates one goal probability above the threshold for providing autonomy assistance, and after the assistance kicks in the subject elects to stop issuing control commands.

This highlights the need for greater transparency in the human-robot interaction, so that the human has a clear picture of how and why the robot chooses to help the user in certain ways. A lack of understanding of how they might help the robot to help them might have resulted in the under-utilization of the disambiguation feature. In order to provide intent-expressive control commands to the robot, very likely knowledge of the assistance mechanism is critical. Therefore, the need for extensive and thorough training becomes apparent. The training can be made more effective in a few different ways. First, online feedback of the robot's intent prediction at all times during training can likely help the subject gain a better understanding of the relationship between the characteristics of their control actions (sparsity, aggressiveness, persistence) and the robot's assistive behavior. Second, the subjects could be explicitly informed of the task relevant features (directedness, proximity et cetera) that the robot relies on for determining the amount of assistance. Knowledge of these features might motivate the users to leverage the disambiguating mode.

The inherent time delays associated with the computation of the disambiguating mode (approximately 2-2.5s) might have been a discouraging factor and a cause for user frustration. The algorithm could be used to pre-compute a large set of most informative modes for different parts of the workspace, goal configurations and priors ahead of time, which then might be used a lookup table during task execution. Furthermore, metamodeling techniques and machine learning tools can be

used to learn generalizable models that will be effective in previously unseen goal configurations.

Automated mode switching schemes that eliminate the need for manual button presses altogether might also be a viable option for reducing task effort significantly.

VIII. CONCLUSION

In this paper, we have presented an algorithm for *intent disambiguation assistance* with a shared-control robotic arm using the notion of *inverse legibility*. The goal of our algorithm is to elicit more *intent-expressive* control commands from the user by placing control in those control modes that *maximally disambiguate* between the various goals in the scene. As a secondary contribution, we also present a novel intent inference mechanism inspired by *dynamic field theory* that works in conjunction with the disambiguation system. A pilot user study was conducted with eight subjects to evaluate the efficacy of the disambiguation system. Our results indicate a decrease in task effort in terms of the number of button presses when disambiguation system employed.

In our future work, as informed by our pilot study, we plan to extend the framework into an automated mode switch assistance system. A more extensive user study with motorimpaired subjects will also be conducted in the future to further evaluate the utility of the disambiguation system and explore the disambiguation request patterns of users.

ACKNOWLEDGMENT

This material is based upon work supported by the National Science Foundation under Grant CNS 1544741. Any opinions, findings and conclusions or recommendations expressed in this material are those of the authors and do not necessarily reflect the views of the aforementioned institutions.

REFERENCES

- [1] M. P. LaPlante *et al.*, "Assistive technology devices and home accessibility features: prevalence, payment, need, and trends." *Advance Data from Vital and Health Statistics*, 1992.
- [2] L. V. Herlant, R. M. Holladay, and S. S. Srinivasa, "Assistive teleoperation of robot arms via automatic time-optimal mode switching," in *Proceedings* of the ACM/IEEE International Conference on Human-Robot Interaction (HRI), 2016.
- [3] J. Philips, J. d. R. Millán, G. Vanacker, E. Lew, F. Galán, P. W. Ferrez, H. Van Brussel, and M. Nuttin, "Adaptive shared control of a brainactuated simulated wheelchair," in *Proceedings of the IEEE International Conference on Rehabilitation Robotics (ICORR)*. IEEE, 2007, pp. 408–414.
- [4] E. Demeester, A. Hüntemann, D. Vanhooydonck, G. Vanacker, H. Van Brussel, and M. Nuttin, "User-adapted plan recognition and user-adapted shared control: A bayesian approach to semi-autonomous wheelchair driving," *Autonomous Robots*, vol. 24, no. 2, pp. 193–211, 2008.
- [5] D. Gopinath, S. Jain, and B. D. Argall, "Human-in-the-loop optimization of shared autonomy in assistive robotics," *IEEE Robotics and Automation Letters*, vol. 2, no. 1, pp. 247–254, 2017.
- [6] K. Muelling, A. Venkatraman, J.-S. Valois, J. E. Downey, J. Weiss, S. Javdani, M. Hebert, A. B. Schwartz, J. L. Collinger, and J. A. Bagnell, "Autonomy infused teleoperation with application to brain computer interface controlled manipulation," *Autonomous Robots*, pp. 1–22, 2017.

- [7] P. M. Pilarski, M. R. Dawson, T. Degris, J. P. Carey, and R. S. Sutton, "Dynamic switching and real-time machine learning for improved human control of assistive biomedical robots," in *Proceedings of the IEEE RAS & EMBS International Conference on Biomedical Robotics and Biomechatronics (BioRob)*. IEEE, 2012, pp. 296–302.
- [8] C. Liu, J. B. Hamrick, J. F. Fisac, A. D. Dragan, J. K. Hedrick, S. S. Sastry, and T. L. Griffiths, "Goal inference improves objective and perceived performance in human-robot collaboration," in *Proceedings of the 2016 International Conference on Autonomous Agents & Multiagent Systems*. International Foundation for Autonomous Agents and Multiagent Systems, 2016, pp. 940–948.
- [9] Y. S. Choi, C. D. Anderson, J. D. Glass, and C. C. Kemp, "Laser pointers and a touch screen: intuitive interfaces for autonomous mobile manipulation for the motor impaired," in *Proceedings of the International* SIGACCESS Conference on Computers and Accessibility, 2008.
- [10] A. D. Dragan and S. S. Srinivasa, Formalizing assistive teleoperation. MIT Press, 2012.
- [11] S. Javdani, H. Admoni, S. Pellegrinelli, S. S. Srinivasa, and J. A. Bagnell, "Shared autonomy via hindsight optimization for teleoperation and teaming," arXiv preprint arXiv:1706.00155, 2017.
- [12] H. Admoni and S. Srinivasa, "Predicting user intent through eye gaze for shared autonomy," in *Proceedings of the AAAI Fall Symposium Series:* Shared Autonomy in Research and Practice (AAAI Fall Symposium), 2016, pp. 298–303.
- [13] B. D. Ziebart, A. L. Maas, J. A. Bagnell, and A. K. Dey, "Maximum entropy inverse reinforcement learning." in AAAI, vol. 8. Chicago, IL, USA, 2008, pp. 1433–1438.
- [14] A. D. Dragan and S. S. Srinivasa, "A policy-blending formalism for shared control," *The International Journal of Robotics Research*, vol. 32, no. 7, pp. 790–805, 2013.
- [15] J. J. Abbott, P. Marayong, and A. M. Okamura, "Haptic virtual fixtures for robot-assisted manipulation," in *Robotics research*. Springer, 2007, pp. 49–64.
- [16] A. D. Dragan, K. C. Lee, and S. S. Srinivasa, "Legibility and predictability of robot motion," in *Proceedings of the ACM/IEEE International* Conference on Human-Robot Interaction (HRI), 2013.
- [17] R. M. Holladay, A. D. Dragan, and S. S. Srinivasa, "Legible robot pointing," in *The IEEE International Symposium on Robot and Human Interactive Communication (RO-MAN)*, 2014.
- [18] D. Gopinath and B. Argall, "Mode switch assistance to maximize human intent disambiguation," in *Robotics: Science and Systems*, 2017.
- [19] G. Schöner and J. Spencer, Dynamic thinking: A primer on dynamic field theory. Oxford University Press, 2015.
- [20] S.-i. Amari, "Dynamics of pattern formation in lateral-inhibition type neural fields," *Biological Cybernetics*, vol. 27, no. 2, pp. 77–87, 1977.
- [21] H. R. Wilson and J. D. Cowan, "A mathematical theory of the functional dynamics of cortical and thalamic nervous tissue," *Biological Cybernetics*, vol. 13, no. 2, pp. 55–80, 1973.
- [22] G. Schöner, "Dynamical systems approaches to cognition," Cambridge Handbook of Computational Cognitive Modeling, pp. 101–126, 2008.
- [23] S. Jain and B. Argall, "Recursive bayesian human intent recognition in shared-control robotics," in 2018 IEEE/RSJ International Conference on Intelligent Robots and Systems (IROS). IEEE, 2018, pp. 3905–3912.
- [24] B. D. Argall, S. Chernova, M. Veloso, and B. Browning, "A survey of robot learning from demonstration," *Robotics and Autonomous Systems*, vol. 57, no. 5, pp. 469–483, 2009.
- [25] S. Schaal, "Learning from demonstration," in Advances in Neural Information Processing Systems, 1997, pp. 1040–1046.
- [26] D. Hsu, R. Kindel, J.-C. Latombe, and S. Rock, "Randomized kinodynamic motion planning with moving obstacles," *The International Journal of Robotics Research*, vol. 21, no. 3, pp. 233–255, 2002.
- [27] N. Ratliff, M. Zucker, J. A. Bagnell, and S. Srinivasa, "Chomp: Gradient optimization techniques for efficient motion planning," in *Proceedings of the IEEE International Conference on Robotics and Automation (ICRA)*. IEEE, 2009, pp. 489–494.
- [28] E. Rimon and D. E. Koditschek, "Exact robot navigation using artificial potential functions," *IEEE Transactions on Robotics and Automation*, vol. 8, no. 5, pp. 501–518, 1992.
- [29] H. G. Tanner, S. G. Loizou, and K. J. Kyriakopoulos, "Nonholonomic navigation and control of cooperating mobile manipulators," *IEEE Transactions on Robotics and Automation*, vol. 19, no. 1, pp. 53–64, 2003.
- [30] O. Khatib, "Real-time obstacle avoidance for manipulators and mobile robots," *The International Journal of Robotics Research*, vol. 5, no. 1, pp. 90–98, 1986.